	to be zero	[sec]
θ_m	= θ at H in Fig. 2, waiting time for homogeneous nucleation	[sec]
σ	= surface energy	[erg/cm^2]

Literature Cited

1) Harano, Y., K. Nakano, M. Saito and T. Imoto: *J. Chem. Eng. Japan*, **9**, 373 (1976).
2) Harano, Y. and K. Oota: *ibid.*, **11**, 119 (1978).
3) *idem*: *ibid.*, **11**, 159 (1978).
4) Mullin, J. W.: "Crystallization", 2nd ed., p. 142, Butterworth Co., London, England (1972).
5) Nývlt, J.: *J. Crystal Growth*, **3/4**, 377 (1969).

(Presented at the Symposium on Crystallization, at Nagoya, April 1978.)

LIQUID-SOLID MASS TRANSFER IN GAS-LIQUID COCURRENT FLOWS THROUGH BEDS OF SMALL PACKINGS

MAMORU YOSHIKAWA, KATSUSHI IWAI, SHIGEO GOTO AND HIDEO TESHIMA
Department of Chemical Engineering, Nagoya University, Nagoya 464

Rates of mass transfer from liquid phase to small particles (average diameter, 0.46–1.3 mm) were measured by use of ion-exchange reaction followed by instantaneous irreversible reaction at 30°C. Nitrogen gas and dilute aqueous solution of sodium hydroxide were fed into a shallow bed packed with a strong cation exchange resin. Volumetric mass transfer coefficients for gas-liquid cocurrent upflow and downflow were almost identical at the same gas and liquid flowrates but became somewhat greater than those in liquid-full single phase flow. A unified correlation could be derived by arranging experimental data for three arrangements: liquid-full single phase flow, gas-liquid cocurrent upflow and downflow (trickle-bed).

Introduction

Mass transfer between a flowing liquid and a bed packed with solid particles in the presence of a cocurrently flowing gas is of concern in a variety of chemical engineering applications as described in a recent book[18]. Many data and correlations on liquid-solid mass transfer in packed beds are available for gas-liquid two-phase cocurrent upflow[3,15] and downflow[4,7,9,16,17,22] as well as liquid-full single phase flow[1,5,6,10,14,21,23]. The diameters of particles are larger than 3 mm in most of the literature.

Little attention has so far been given to beds of small packings. Diffusional resistances may be significant in the pores of catalyst particles, which are completely filled with liquid due to capillary force[2]. Therefore, small particles may have some advantages in packed-bed reactor performance, although the pressure drop increases.

Experimental data on liquid-solid mass transfer have been obtained mainly from dissolution of slightly soluble particles such as naphthalene and benzoic acid into flowing water[8-9,14,16,17,20,22]. For small particles, however, the diameters of particles change rapidly due to their large external surface, and the measurements may be inaccurate. It is more suitable to use ion-exchange reactions with small resin particles whose diameters do not change significantly during reactions. Some data have been published for liquid-full single phase flow[10,21].

In this study, to obtain correlations of liquid-solid mass transfer in beds packed with small particles, mass transfer rates of Na^+ ion from aqueous solution of NaOH to resin particles are measured in shallow beds for three arrangements; gas-liquid cocurrent upflow, downflow (trickle-bed) and liquid-full single flow. Direct comparison among different flow arragements in the same apparatus[7,20] may be valuable for the design of three-phase packed-bed reactors.

1. Evaluation of Mass Transfer Coefficients

If an aqueous solution of NaOH contacts a strong cation-type resin, the ion-exchange reaction is fol-

Received March 2, 1981. Correspondence concerning this article should be addressed to S. Goto. M. Yoshikawa is now with Kao Soap Co., Ltd., Kashima 314-02.

lowed by an instantaneous irreversible reaction, i. e. neutralization. The consecutive reactions can be expressed by the following equation.

$$R\text{-}H^+ + NaOH \longrightarrow R\text{-}Na^+ + H_2O \quad (1)$$

Mass balance equations for NaOH in a packed bed with negligible axial dispersion are:

$$u_L \frac{\partial C}{\partial z} + \varepsilon_L \frac{\partial C}{\partial t} + \rho_B \frac{\partial q}{\partial t} = 0 \quad (2)$$

$$\rho_B \frac{\partial q}{\partial t} = (ka)_s (C - C_s) \quad (3)$$

Equation (3) holds under the unsaturated condition of $q<Q$. When the concentration in the resin phase, q, attains the capacity of the resin, Q, the accumulation term, $\rho_B \partial q/\partial t$ in Eq. (2) vanishes.

For the case of liquid-film rate controlling, the concentration of NaOH at the solid-liquid interface, C_s is always zero. Also, the volumetric mass transfer coefficient, $(ka)_s$ for ion exchange in a base or acid may be constant through the reaction in contrast to the case of ion exchange in a salt solution[10].

The breakthrough curve can be obtained analytically[11] from Eqs. (2) and (3) and is divided into three periods as follows.

(a) Unsaturated period $(0<\tau<1)$

$$C_{out}/C_{in} = \exp(-\xi) \quad (4)$$

(b) Partially saturated period $(1 \leq \tau < \xi + 1)$

$$C_{out}/C_{in} = \exp(\tau - \xi - 1) \quad (5)$$

(c) Completely saturated period $(\tau \geq \xi + 1)$

$$C_{out}/C_{in} = 1 \quad (6)$$

The time when saturation starts, t_s, can be determined from $\tau = 1$.

$$t_s = \rho_B Q / \{(ka)_s C_{in}\} + \varepsilon_L z_t / u_L \quad (7)$$

For the shallow bed, the second term of the right-hand side in Eq. (7) may be negligible because z_t is small.

Since the concentration at the outlet, C_{out} is independent of time in the unsaturated period, the coefficient $(ka)_s$ can be derived from Eq. (4) as

$$(ka)_s = u_L \xi / z_t = (u_L / z_t) \ln (C_{in}/C_{out});\ 0 < t < t_s \quad (8)$$

On the other hand, when resin particles are packed in the shallow bed, the average concentration $C_{av} = (C_{in} + C_{out})/2$ may be used in mass balance equations, and then the coefficient $(ka)_s$ can be given as

$$(ka)_s = (u_L/z_t)(C_{in} - C_{out})/C_{av} \quad (9)$$

If the concentration at the outlet, C_{out}, is greater than $C_{in}/2$, the difference between $(ka)_s$ from Eq. (8) and that from Eq. (9) is within 4%.

2. Experimental Apparatus and Procedure

Figure 1 shows the details of the packed bed arrangements for gas-liquid cocurrent upflow and

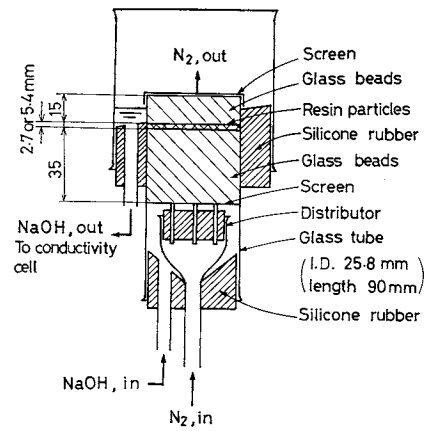

Fig. 1 Packed bed arrangement for cocurrent upflow

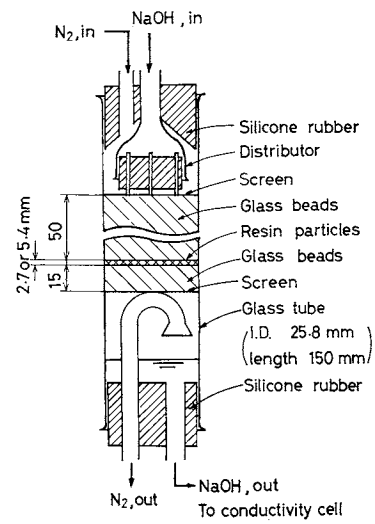

Fig. 2 Packed bed arrangement for cocurrent downflow

liquid-full single flow. The depth of the shallow bed packed with ion-exchange resins was 2.7 or 5.4 mm in a 25.8 mm I.D. glass tube. Glass beads of almost the same diameter as the resin particles were used to calm gas and liquid flows.

Stainless steel screens were placed at the top and bottom of the bed to prevent the movement of particles. Aqueous solution of NaOH and N_2 gas were separated over the shallow bed in a 50 mm I.D. glass tube. The gas was introduced through a distributor containing five capillary tubes (1 mm I.D. and 10 mm in length). All apparatus was immersed in a thermostat at 30°C.

For downflow operation, the same 25.8 mm I.D. glass tube was used with the distributor, now used for liquid, placed at the top of the bed as shown in **Fig. 2.** The liquid and gas streams were separated at the bottom of the bed.

Auxiliary apparatus included a feed reservoir of NaOH solution and a N_2 gas cylinder followed by appropriate regulators for controlling liquid and gas streams. The feed concentration of NaOH was

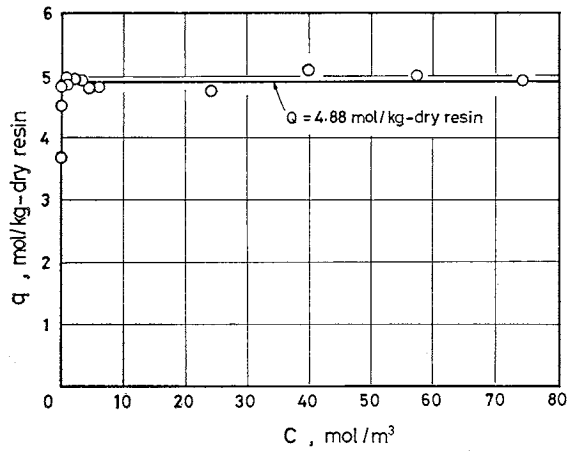

Fig. 3 Equilibrium relationship of NaOH at 30°C

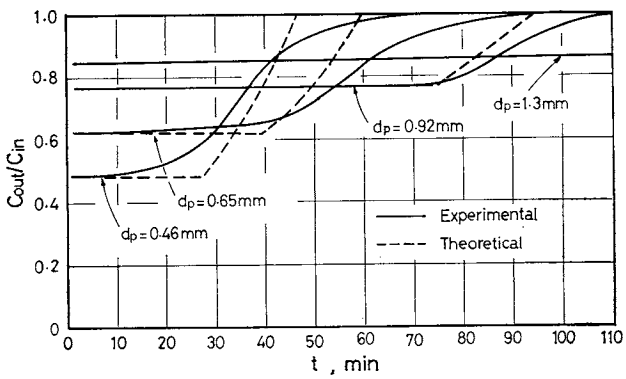

Fig. 4 Breakthrough curves in shallow bed

0.1 or 1 mol/m³.

Amberlyst 15, designated as a macroreticular (MR) ion-exchanger[13], was used as a strong cation exchange resin for the reactions described in Eq. (1). The swollen resins were sieved in water. Four fractions of 12 to 14, 16 to 20, 24 to 28 and 32 to 35 mesh sizes were chosen and average diameters of particles, d_p, were calculated from the arithmetic averages of openings of two sieves as 1.3, 0.92, 0.65 and 0.46 mm, respectively. The measured values of ρ_B, ε_B and ω were 745 kg-swollen resin/m³, 0.371 and 0.528, respectively. The specific area a_t was calculated from $a_t=6(1-\varepsilon_B)/d_p$.

At first, a bed packed with H^+ type Amberlyst 15 was filled with distilled water and then NaOH solution and N_2 gas were fed to the bed at given flowrates. The concentrations of NaOH at the inlet and outlet were measured continuously by a flowthrough electric conductivity cell at the feed line to the shallow bed and the exhaust line from the separator, respectively. Nitrogen gas did not disturb the readings of electric conductivity in the liquid phase.

3. Preliminary Experimental Results

3. 1 Equilibrium relationship

Test tubes containing NaOH solution and swollen resin of Amberlyst 15 were immersed in a themostat at 30°C for about 100 hours. The concentration of NaOH in the liquid phase, C, was measured by an electric conductivity meter and the concentration in the resin phase, q, was calculated from the difference between initial and final concentrations of NaOH in the liquid phase.

The results for equilibrium data are shown in the circles in **Fig. 3.** As expected, the equilibrium relationship becomes a rectangular type and the concentration in the liquid phase, C, is nearly zero within the capacity of the resin. The solid line in Fig. 3 indicates the capacity of the resin, Q, which was determined by the column method[12] to be 4.88 mol/kg-dry resin.

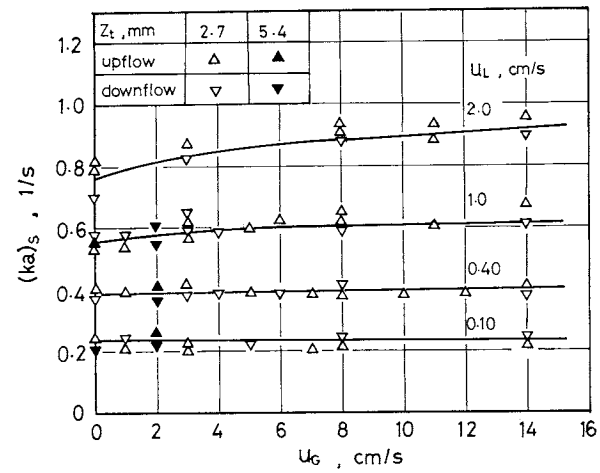

Fig. 5 Volumetric liquid-solid mass transfer coefficients for both upflow and downflow at d_p= 0.92 mm

3. 2 Breakthrough curves

Experimental breakthrough curves for liquid-ful single flow of $C_{in}=1$ mol/m³ in the shallow bed of $z_t=$ 2.7 mm are shown in the solid lines in **Fig. 4** for four sizes of resin particles. The values of $(ka)_s$ calculated from Eq. (9) were constant in the initial period for two larger sizes ($d_p=1.3$ and 0.92 mm) while these were decreased with time for two smaller sizes ($d_p=0.65$ and 0.46 mm).

Dotted lines in Fig. 4 show theoretical breakthrough curves obtained from Eqs. (4)–(6) by using the values of $(ka)_s$ extrapolated to $t=0$. The agreement between experimental and theoretical curves is excellent in the unsaturated period for the two larger sizes. The disagreement in other conditions may be due to shorter unsaturated period and the mixing of liquid phase in the separator.

If feed concentration C_{in} decreases, time t_s in Eq. (7) can be increased. Therefore, when $C_{in}=0.1$ mol/m³, good agreement between experimental and theoretical curves was obtained in the unsaturated period for the two smaller sizes.

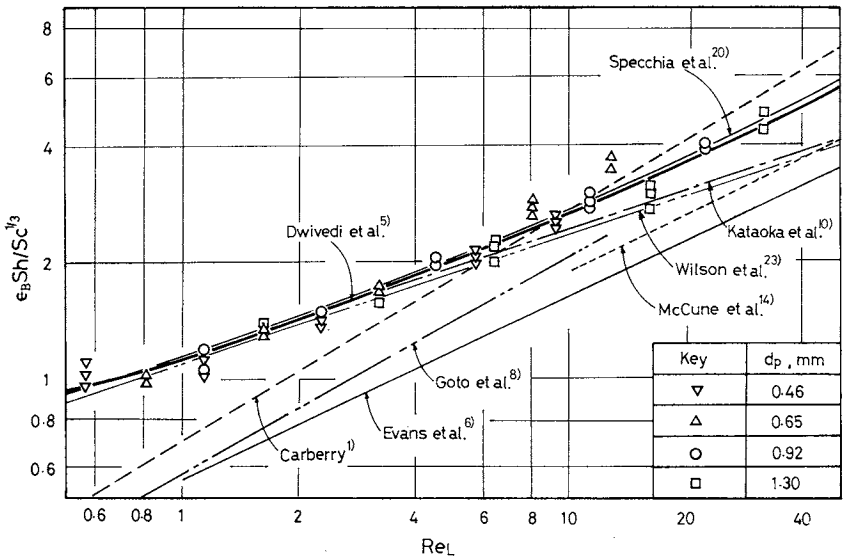

Fig. 6 Liquid-solid mass transfer correlations for liquid-full single flow

Similar results were obtained for gas-liquid cocurrent upflow and downflow in various conditions.

4. Experimental Values of $(ka)_s$

It is evident from the results of the equilibrium relationship and breakthrough curves in the previous section that the assumption of zero concentration of NaOH at the liquid-solid interface ($C_s=0$) should be satisfied in the unsaturated period ($0<t<t_s$). Thus, the values of $(ka)_s$ could be calculated by Eq. (9) from the experimental data of $C_{out}>C_{in}/2$ in the unsaturated period.

Gas and liquid flowrates were in the ranges of 0–14 cm/s and 0.1–2 cm/s, respectively.

Figure 5 shows the effects of gas flowrate u_G on $(ka)_s$ for various values of liquid flowrate u_G and one particle size, $d_p=0.92$ mm. In this figure, data of upflow at $u_G=0$ correspond to liquid-full operation while those of downflow at $u_G=0$ correspond to trickle-bed operation because the gas phase still exists. The values of $(ka)_s$ for cocurrent upflow were almost the same as those for cocurrent downflow. No end effects were found since there were no differences between data from $z_t=2.7$ mm and those from $z_t=5.4$ mm. The values of $(ka)_s$ were nearly insensitive to the gas flowrate, u_G, although small effects appeared at $u_L=1.0$ and 2.0 cm/s. The solid lines represent the values calculated from Eq. (12), as will be developed later.

Similar experimental results were obtained for other particle sizes, $d_p=0.46$, 0.65 and 1.3 mm.

5. Comparison with Previous Correlations

To compare our data with published correlations, $\varepsilon_B Sh/Sc^{1/3}$ was plotted versus Re_L for three arrangements. The molecular diffusivity of NaOH in very dilute aqueous solution was estimated by the equation (Eq. (2.37) in Sherwood *et al.*[19]) as $D_L=2.13\times10^{-9}$m^2/s at 25°C. The empirical relation $D_L\mu_L/T$ was used to obtain $D_L(=2.41\times10^{-9}$m^2/s) at 30°C. Other physical properties at 30°C were determined from those of N_2 gas and pure water as $\rho_G=1.13$ kg/m^3, $\mu_G=1.80\times10^{-5}$ kg/m s, $\rho_L=0.996\times10^3$ kg/m^3 and $\rho_L=8.02\times10^{-4}$ kg/m·s. Then, Schmidt number, Sc $(=\mu_L/\rho_L D_L)$, was determined as 334.2. J_D factor, which was adopted in many papers[1,4–6,8,14,23], was converted to Sherwood number by the relation $Sh/Sc^{1/3}=Re_L J_D$. The value of ε_B was fixed at 0.371, as measured in our experiments.

5. 1 Liquid-full single phase flow

The experimental results for four particle sizes in liquid-full single phase flow are shown in **Fig. 6** together with many published correlations. Most of our data are on the line of the correlation proposed by Dwivedi and Upadhyay[5], who reanalyzed previous experimental data on mass transfer between liquid and solid in fixed and fluidized beds. The correlation equation is given as

$$\varepsilon_B Sh/Sc^{1/3}=0.765Re_L^{0.18}+0.365Re_L^{0.614} \qquad 10^{-3}<Re_L<10^4 \tag{10}$$

Other correlations gave lower values than our experimental data, except that of Specchia *et al.*[20].

5. 2 Gas-liquid cocurrent upflow

Figure 7 shows some published correlations for gas-liquid cocurrent upflow and also our data at the highest gas flowrate ($u_G=14.0$ cm/s) in our experiments. As Re_L increases, our experimental data become greater than values estimated from Eq. (10) for single-phase flow.

The correlations of Specchia *et al.*[10] and Mochizuki[15] were determined from data for larger particles $d_p\geq6$ mm) and the mass transfer coefficients in upflow operation increased up to 5 times those in liquid-

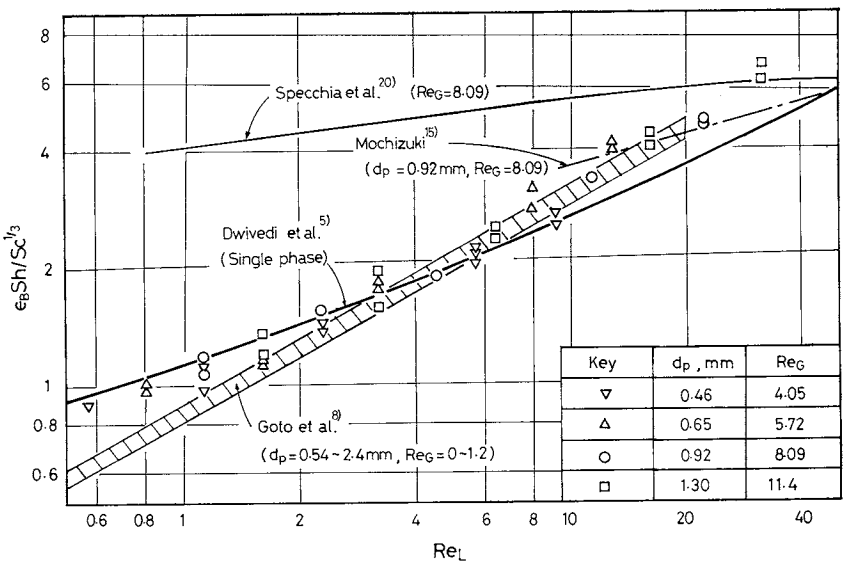

Fig. 7 Liquid-solid mass transfer correlations for gas-liquid cocurrent upflow

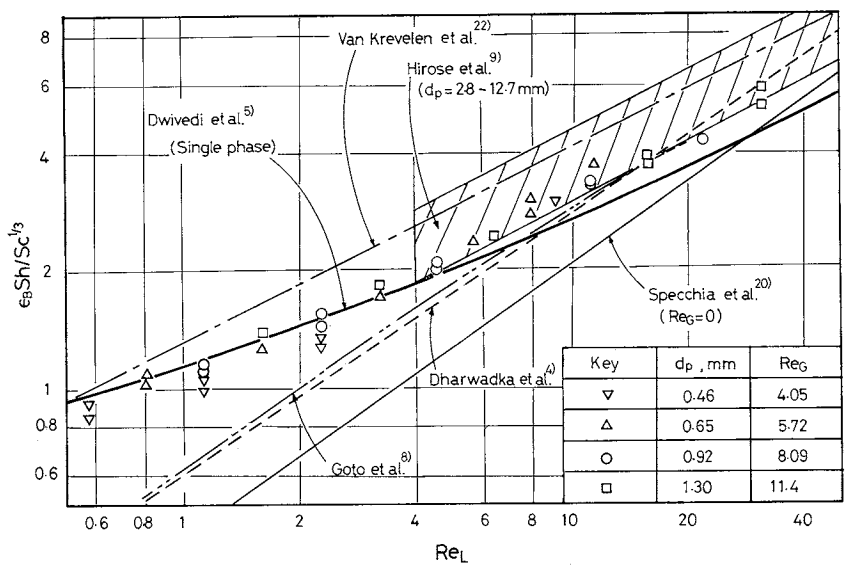

Fig. 8 Liquid-solid mass transfer correlations for gas-liquid cocurrent downflow

full operation as a function of Re_L/Re_L or $d_p^{1.2}Re_G^{0.55}/Re_L^{0.77}$. The values in Fig. 7 were obtained by extrapolating to the case of d_p=0.92 mm and Re_G=8.09. These correlations give higher values than our data for lower values of Re_L. On the other hand, the data of Goto *et al.*[8] for d_p=0.54–2.4 mm and Re_G=0–1.2 are almost identical to our data.

5. 3 Gas-liquid cocurrent downflow

Experimental data for gas-liquid cocurrent downflow with u_G=14.0 cm/s are shown in **Fig. 8** together with published correlations. Our data have the same tendencies as those for upflow operation.

The correlation of Van Krevelen and Krekels[22] and data of Hirose *et al.*[9] give higher values than our data while the correlations of Dharwadkar and Sylvester[4], Goto *et al.*[8] and Specchia *et al.*[20] give lower values.

6. Unified Correlation

The enhancement factor, β, was defined by Hirose *et al.*[9] as the ratio of $(ka)_s$ in cocurrent flow to that in single-phase flow at the same liquid flowrate.

It varied from 1.2 to 2.0 in trickle-bed reactors packed with spheres of 2.8–12.7 mm.

As described in previous sections, the values of $(ka)_s$ in both upflow and downflow were somewhat greater than in single-phase flow at higher values of Re_L and Re_G in a bed packed with small-diameters packing. The value of β was determined from the ratio of $(ka)_s$ in cocurrent flow to that calculated from the correlation for single phase flow, Eq. (10). The enhancement factor, β could be expressed as functions of $\sqrt{Re_G}$ and Re_L by

$$\beta=1+0.003\,Re_L\sqrt{Re_G} \qquad (11)$$

More than 500 points for various gas and liquid flowrates and four sizes of packings were included in the plot of $(\varepsilon_B Sh/Sc^{1/3})/\beta$ vs. Re_L shown in **Fig. 9**. Most points fall within 20% of the value calculated by

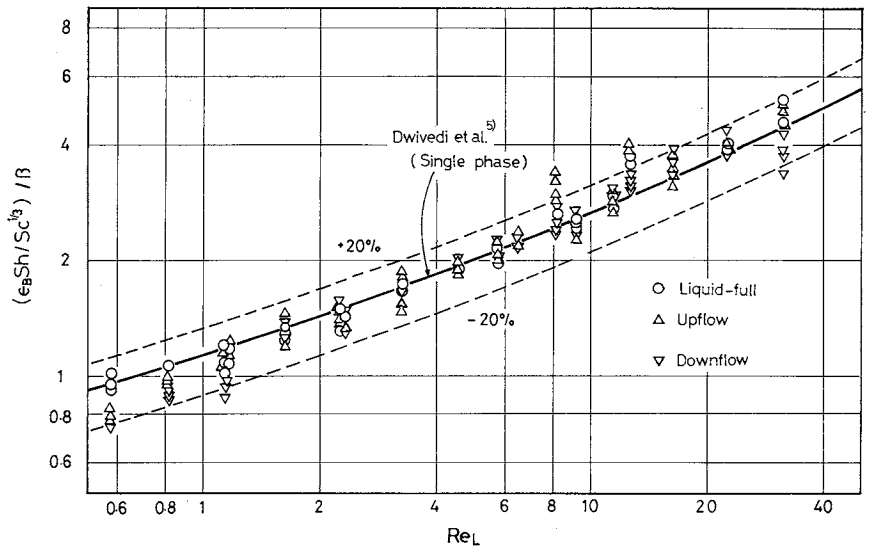

Fig. 9 Unified correlation for three arrangements

Eq. (10). Therefore, the unified correlation may be expressed as

$$\varepsilon_B Sh/Sc^{1/3}=(1+0.003Re_L\sqrt{Re_G})(0.765\ Re_L^{0.18}+0.365Re_L^{0.614});$$

$$0.46<d_p<1.3\text{ mm},\ 0<Re_G<12,\ 0.5<Re_G<50 \quad (12)$$

For liquid-full operation ($Re_L=0$), Eq. (12) can be reduced to Dwivedi and Upadhyay's equation, that is, Eq. (10). The solid lines in Fig. 5 were determined from Eq. (12) and agree well with experimental data.

Conclusions

The rates of liquid-solid mass transfer in packed beds with gas-liquid cocurrent flow were measured by using ion-exchange reaction followed by instantaneous irreversible reaction at 30°C. Nitrogen gas and NaOH solution were fed into a shallow bed packed with small particles (d_p=0.46–1.30 mm) of macroreticular ion-exchange resin, Amberlyst 15.

The volumetric mass transfer coefficients, $(ka)_s$, in upflow and downflow operations were almost identical at the same gas and liquid flowrates but became somewhat greater than those in liquid-full operation. When the enhancement factor β was introduced, most of our experimental data could be correlated by Eq. (12), which was based on Dwivedi and Upadhyay's correlation for single flow.

Nomenclature

a_t	=	total external surface area of particles per unit volume of bed	[1/m]
C	=	concentration of NaOH in liquid phase	[mol/m³]
D_L	=	molcular diffusivity of NaOH in liquid phase	[m²/s]
d_p	=	particle diameter	[m]
J_D	=	$(ka)_s Sc^{2/3}/(u_L a_t)$	[—]
$(ka)_s$	=	volumetric mass transfer coefficient in liquid-to-solid transport	[1/s]
Q	=	resin capacity	[mol/kg-dry resin]
q	=	concentration of NaOH in resin phase	[mol/kg-dry resin]
Re	=	Reynolds number, $d_p\rho u/\mu$	[—]
Sc	=	Schmidt number, $\mu_L/(\rho_L D_L)$	[—]
Sh	=	Sherwood number, $(ka)_s d_p/(a_t D_L)$	[—]
T	=	temperature	[K]
t	=	time	[s]
t_s	=	time when saturation starts, defied by Eq. (7)	[s]
u	=	superficial velocity	[m/s]
z	=	axial coodinate	[m]
z_t	=	total depth of bed	[m]
β	=	enhancement factor defined by Eq. (11)	[—]
ε_B	=	void fraction in bed	[—]
ε_L	=	liquid hold-up	[—]
μ	=	fluid viscosity	[kg/m·s]
ξ	=	$(ka)_s z_t/u_L$	[—]
ρ	=	fluid density	[kg/m³]
ρ_B	=	bed density	[kg/m³]
τ	=	$(ka)_s C_{in}(t-\varepsilon_L z_t/u_L)/(\rho_B Q)$	[—]
ω	=	weight fraction of water in resin	[—]

〈Subscripts〉

G	=	gas phase
in	=	inlet
L	=	liquid phase
out	=	outlet

Literature Cited

1) Carberry, J. J.: *AIChE J.*, **6**, 460 (1960).
2) Colombo, A. J., G. Baldi and S. Sicardi: *Chem. Eng. Sci.*, **31**, 1101 (1976).
3) Delaunay, G., A. Storck, A. Laurent and J. C. Charpentier: *Ind. Eng. Chem., Process Des. Develop.*, **19**, 514 (1980).
4) Dharwadkar, A. and N. D. Sylvester: *AIChE J.*, **23**, 376 (1977).
5) Dwivedi, P. N. and S. N. Upadhyay: *Ind. Eng. Chem., Process Des. Develop.*, **16**, 157 (1977).
6) Evans, G. C. and C. F. Gerald: *Chem. Eng.*, **49**, 191 (1953).
7) Goto, S. and J. M. Smith: *AIChE J.*, **21**, 706 (1975).
8) Goto, S., J. Levec and J. M. Smith: *Ind. Eng. Chem., Process Des. Develop.*, **14**, 473 (1975).
9) Hirose, T., Y. Mori and Y. Sato: *J. Chem. Eng. Japan*, **9**,

220 (1976).
10) Kataoka, T., N. Sato and K. Ueyama: *ibid.*, **1**, 38 (1968).
11) Kataoka, T. and H. Yoshida: *ibid.*, **9**, 326 (1976).
12) Kawabe, T., H. Teshima and N. Morita: *Kogyo Kagaku Zasshi*, **70**, 133 (1967).
13) Kunin, R., E. Meitzner, J. A. Oline, S. Fisher and N. Frisch: *Ind. Eng. Chem., Prod. Res. Develop.*, **1**, 140 (1962),
14) McCune, L. and R. H. Wilhelm: *Ind. Eng. Chem.*, **41**, 1124 (1949).
15) Mochizuki, S.: *AIChE J.*, **24**, 1138 (1978).
16) Ruether, J. A., C. S. Yang and W. Hayduk: *Ind. Eng. Chem., Process Des. Develop.*, **19**, 103 (1980).
17) Satterfield, C. N., M. W. Van Eek and G. S. Bliss: *AIChE J.*, **24**, 709 (1978).
18) Shah, Y. T.: "Gas-Liquid-Solid Reactor Design", pp. 180–274, McGraw Hill (1979).
19) Sherwood, T. K., R. L. Pigford and C. R. Wilke: "Mass Transfer", p. 35, McGraw Hill (1975).
20) Specchia, V., G. Baldi. and A. Gianetto: *Ind. Eng. Chem., Process Des. Develop.*, **17**, 362 (1978).
21) Tien, C. and G. Thodos: *Chem. Eng. Sci.*, **13**, 120 (1960).
22) Van Krevelen, D. W. and J. T. C. Krekeles: *Rec. Trav. Chim.*, **67**, 512 (1948).
23) Wilson, E. J. and J. Geankoplis: *Ind. Eng. Chem., Fundam.*, **5**, 9 (1966).

(Presented in part at the 12th Autumn Meeting of The Soc. of Chem. Engrs., Japan, at Okayama, October, 1978.)

EFFECT OF SINTERING ON THE REACTION RATE IN A GAS-SOLID REACTION SYSTEM

NOBORU SAKAI, TADASHI CHIDA AND TEIRIKI TADAKI
Department of Mining and Mineral Engineering, Tohoku University, Sendai 980

Effect of sintering on the reaction rate in a gas-solid system is discussed theoretically with a mathematical model, in which it is assumed that a solid pellet consists of a large number of fine particles, and that the pellet radius becomes smaller by a factor of β than that of theoretical one owing to sintering. The model clarifies quantitatively the deceleration mechanism of overall reaction rate at the later stage due to decrease of effective diffusivity of gases in the product layer. The theoretical results using this model are compared with experimental ones for the reduction of nickel oxide pellets with hydrogen. The values of β are 0.97 to 0.67 in the temperature range of 673 to 1073 K.

Introduction

In a gas-solid reaction system, solid structural changes which result in swelling, shrinking, cracking and sintering usually take place during the course of reaction. These changes are in general so complicated that the reaction rate may not be treated quantitatively. Sintering is a particularly important factor, because the reaction is usually carried out at elevated temperatures. Sintering of a product layer may affect the overall reaction rate because it suppresses diffusion rate of reactant or product gases through the layer. Such findings have been reported for reduction of nickel oxide with hydrogen[8], and for hydrofluorination of uranium dioxide[1].

The reaction kinetics in such systems have been analyzed by the so-called particle pellet model[2-4,7], a kind of structural model. Using this model, Ramachandran and Smith[5] have interpreted the effect of sintering on the overall reaction rate in terms of removal of pore interconnections. Ranade and Harrison[6] have interpreted it in terms of change rates of specific surface area which result in a decrease in number of particles by sintering. In both models, pellet volume was assumed to be constant. This assumption, however, is unreasonable if sintering is very effective.

In this paper, in addition to the volume change of particles, that of a pellet is considered. A new parameter, the shrinking parameter, is introduced to the particle pellet model in order to explain the effect of sintering on the overall reaction rate. This model is compared with the experimental results of reduction of nickel oxide with hydrogen. And it is shown that the effect of sintering can be explained quite well by use of the parameter.

1. Mathematical Model

Consider a spherical pellet of radius R_0 consisting of nonporous spherical particles of radius r_0 as shown

Received January 23, 1981. Correspondence concerning this article should be addressed to N. Sakai. T. Tadaki is at Dept. of Chem. Eng., Tohoku Univ., Sendai 980.